SNOWDRIFT MODELING USING A LINEAR PARTICLE DISTRIBUTION EQUATION

Noriaki Ohara[1]

ABSTRACT

A snowdrift is affected by numerous factors including but not limited to wind field, local turbulence, boundary layer thickness, surface roughness, particle Reynolds number, snow particle size distribution, particle shape, and density of snow particles in the air. Therefore, snow redistribution has been ignored in most practical hydrology models, and snowdrifts around well-defined snow fences have been projected mainly by empirical knowledge rather than process-based considerations. This study organized these various effects by particle motion processes rather than flow (wind) regime and particle characteristics in order to develop a predictive model for snow redistribution. The particle motion processes were characterized by three parameters: snow particle dispersion, snow drift (snow surface advection), and snow surface erosion coefficients. Among them, a linear erosion term for a fetch-eddy effect was the new addition to the existing advection dispersion equation. The newly formulated equation was named Eulerian Particle Distribution (EPD) equation, and the linear components of the EPD equation were named the Linear Particle Distribution (LPD) equation. Using analytical solutions under a few well-defined boundary conditions, possible snow particle distribution patterns were successfully mapped. The LPD equation was found to be able to describe most of the one-dimensional particle deposit patterns behind an object, including porous and solid snow fences and a tree. The snow redistribution model based on the LPD theory also reproduced snow stratigraphy observed by ground penetrating radar (GPR). Inversely, this theory may provide us an opportunity to estimate the time-averaged particle motion parameters, such as diffusion, drift, and erosion coefficients, from field-observed particle distributions. The model applications and numerical algorithm for snow drift patterns in irregular terrain will be presented. (KEYWORDS: snow drift, Eulerian particle distribution, particle distribution, snow redistribution, snow erosion, snow fence)

INTRODUCTION

Snow redistribution by wind is an important research topic for hydrological model and land surface models as it is difficult to predict the snow patterns around an object such as vegetation and buildings. In fact, many models have just ignored the effect of the wind-snow processes because of our limited understanding of the process. When a snowdrift needs to be estimated, for example, for snow fence design, drift pattern has been mainly predicted by empirical knowledge in practice (e.g. Tabler, 2003). Figure 1 shows a typical snowdrift in leeward of a Wyoming snow fence along the Interstate 80 in Wyoming. Tabler (2003) basically combined the numerous field-observed snowdrift patterns behind snow fences, and developed a methodology based on the measured snowdrift patterns.

Figure 1. Snowdrift in downstream of the Wyoming type snow fence

Paper presented Western Snow Conference 2018
[1] Noriaki Ohara, University of Wyoming, Laramie, WY 82071, nohara1@uwyo.edu

Figure 2. Various snowdrift patterns around non-uniform barriers

Snowdrift shape can be very different depending on types of the object and local wind field. Figure 2 shows another example of snowdrift around a log pile.

Process-based modeling for snowdrift process has remained a challenge although some progress has been made in simplified snow redistribution models, such as: Prairie Blowing Snow Model (PBSM) [Pomeroy et al., 1993; Essery et al., 1999], SnowTran3D [Greene et al., 1999; Liston et al., 2007], and Apine3D [Lehning et al., 2006; Mott et al., 2010]. Micro meteorological wind modification and simple snow transport formulations were implemented in these models. However, the previously available governing equation based on the Eulerian framework, known as Advection-dispersion equation, was insufficient to predict the snowdrift around perforated snow fence. This paper presents the numerical solutions by the new formulation proposed by Ohara (2017).

METHOD

Ohara (2017) derived the governing equation for the dynamic one-dimensional particle distribution as follows,

$$\frac{\partial h}{\partial t} = -\frac{1}{\rho_p}\left[a(x,t)\frac{\partial^2 h}{\partial x^2} + b(x,t)\frac{\partial h}{\partial x} + c(x,t)h + f(x,t)\right] \quad (1)$$

where h is a relative snow surface height [L], $\rho_p$is a density of particle deposit [M/L^3], a is a mass dispersion coefficient [M/T/L], b is a mass advection coefficient [M/T/L^2], c is a mass erosion coefficient [M/T/L^3], and f is a nonlinear and source term (or mathematically, an inhomogeneous term). This equation basically consists of the dispersion, the advection, the erosion, and source terms. These particle motion parameters can be interpreted as,

$$a = -\rho_p D \quad (2)$$
$$b = \rho_p \varphi \quad (3)$$
$$c = \rho_p \varepsilon \quad (4)$$

where D is the surface diffusion coefficient or particle dispersion coefficient [L^2/T], ϕ is the wave migration velocity or celerity [L/T], and ε is the erosion coefficient [1/T]. Among these parameters, the erosion coefficient was newly introduced by Ohara [2017]. This equation is called Eulerian Particle Distribution (EPD) equation, and the linear part of it is called Linear Particle Distribution (LPD) equation in this study. The LPD equation can be solved analytically with appropriate initial and boundary conditions. Particle deposition behind an object can be described by the following initial and boundary conditions (BCs):

$$h(0,t) = h_o U_o(t) \quad (5)$$
$$h(0,t) \neq \infty\,; \quad x \to \infty, t \geq 0 \quad (6)$$
$$h(x,0) = 0\,; \quad x \geq 0 \quad (7)$$

where h_o is a height of the object at x = 0, and $U_o(t)$ is a unit step function. Accordingly, Ohara (2017) derived the exact solution of the LPE as

$$h(x,t) = \frac{h_o}{2}\exp\left(\frac{\varphi x}{2D}\right) \cdot \left[\exp\left(x\sqrt{\frac{\varphi^2}{4D}+\varepsilon}\right)\operatorname{erfc}\left(\sqrt{\frac{1}{4D}}\frac{x}{\sqrt{t}}+\sqrt{\frac{\varphi^2}{4D}+\varepsilon}\cdot\sqrt{t}\right) + \exp\left(-x\sqrt{\frac{\varphi^2}{4D}+\varepsilon}\right)\operatorname{erfc}\left(\sqrt{\frac{1}{4D}}\frac{x}{\sqrt{t}}-\sqrt{\frac{\varphi^2}{4D}+\varepsilon}\cdot\sqrt{t}\right)\right] \tag{8}$$

where

$$\operatorname{erfc}(x) = 1 - \operatorname{erf}(x) \tag{9}$$

This analytical solution of the one-dimensional LPE is convenient for testing the numerical algorithm presented in the later section.

Ohara (2017) also demonstrated that the LPE equation can describe the snowdrift patterns in the downstream area of snow fences, mainly documented by Tabler (2003). Figure 3 shows the synthesized snow accumulation patterns observed and the corresponding predicted snow distributions for various snow fence porosities. This result indicates that the LPD equation can adequately describe the various snowdrift patterns commonly found in nature. It is important to note that the procedure is more than just a fitting exercise because the parameters have physical meaning. The snow dispersion, advection, and erosion coefficients can be estimated from the resultant snow distributions observed. Table 1 shows the fitted model parameters. The advection coefficient *b* does not play an important role in the snowdrift behind the snow fence. The differences in the snow fence porosity influenced both dispersion and erosion coefficients. In particular, the erosion coefficient was found to have clear proportionality to the porosity of the snow fence. Figure 4 explains the fetch/eddy effect described by the linear erosion coefficient *c*. Basically, a positive erosion coefficient yields a monotonous and exponential snowdrift while a negative erosion coefficient results in a snow mound. Accordingly, the erosion coefficient *c* is not only a function of snow surface hardness but also local wind field including eddy.

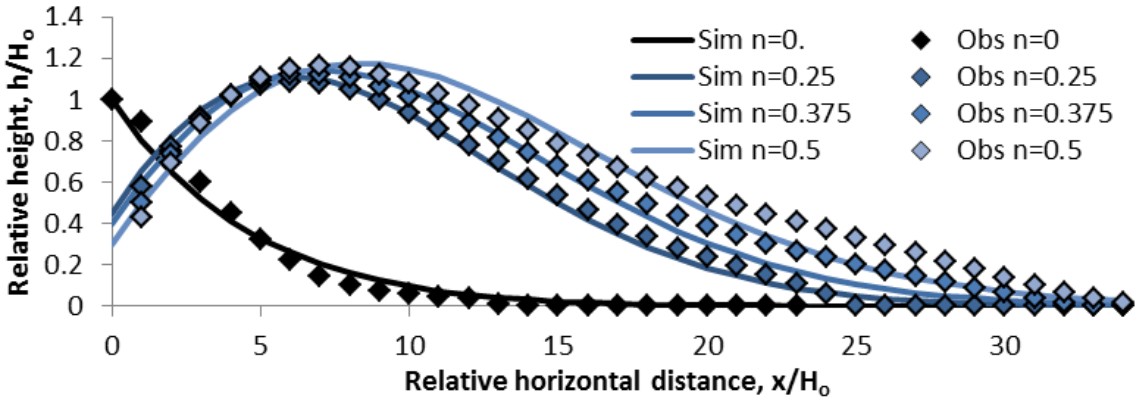

Figure 3. Observed snow profiles behind a Wyoming snow fence (Tabler, 2003) and the fitted solutions for various porosities (Ohara, 2017)

Table 1. Model parameters for four snow fence specifications (Ohara, 2017)

n	-	Porosity of snow fence	**0.5**	**0.375**	**0.25**	**0 (solid fence)**
a	(kg/s/m)	Dispersion	-0.0097	-0.008	-0.00652	-0.0045
b	(kg/s/m^2)	Advection	0	0	0	0
c	(kg/s/m^3)	Erosion	-0.00056	-0.00049	-0.00046	0.0002
ρ_p	(kg/m^3)	Density	360	360	360	360
Δ	(kg^2/s^2/m^4)	Discriminant	-2.17E-05	-1.56E-05	-1.19E-05	3.60E-06

NUMERICAL APPROACH

When a two-dimensional spatial snowdrift patterns over a highly irregular surface topography, a numerical solution is required. The volume-based LPD equation for a two-dimensional spatial field can be written as,

$$\frac{\partial h}{\partial t} = D_x \frac{\partial^2 h}{\partial x^2} - \varphi_x \frac{\partial h}{\partial x} - \varepsilon_x h + D_x \frac{\partial^2 h}{\partial x^2} - \varphi_x \frac{\partial h}{\partial x} - \varepsilon_x h + \frac{f}{\rho_p} \tag{10}$$

where the subscripts denote direction and f is the depth change due to snow precipitation [L/T]. This equation can be discretized with a finite difference-volume mixed method as,

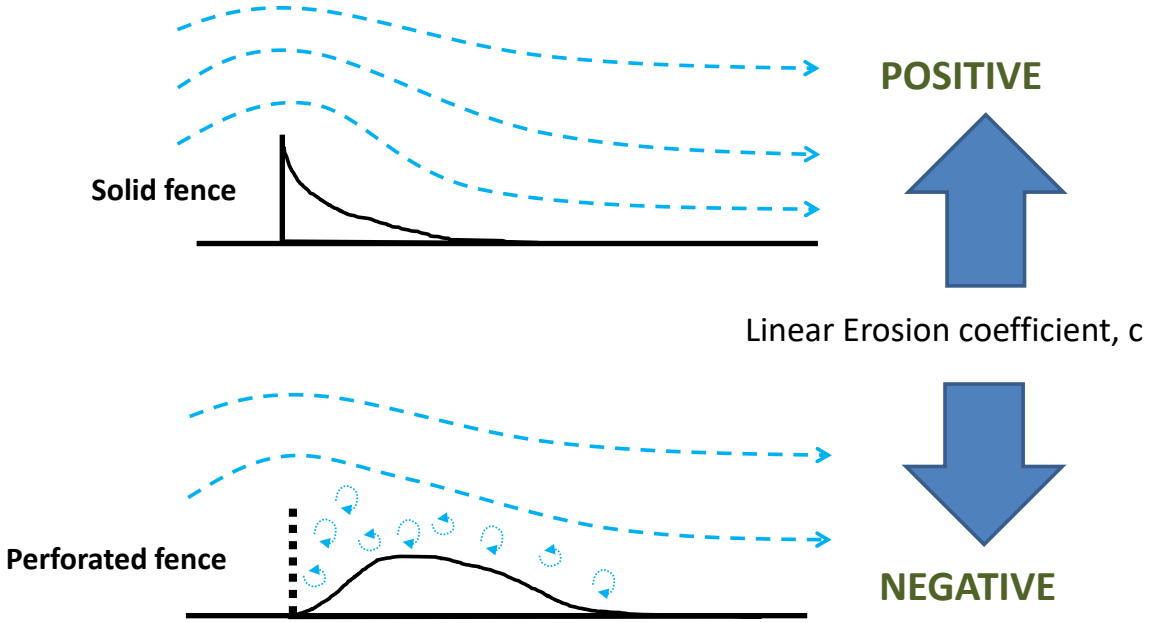

Figure 4. Schematic of fetch/eddy effect linear erosion coefficient

$$h_{i,j}^{n+1} = h_{i,j}^n + D_x \frac{\Delta t}{(\Delta x)^2}\left(h_{i+1,j}^n - 2h_{i,j}^n + h_{i-1,j}^n\right) - \frac{\Delta t}{\Delta x}\left(J^*_{i+\frac{1}{2},j} - J^*_{i-\frac{1}{2},j}\right) - \Delta t \varepsilon_x h_{i,j}^n$$
$$+ D_y \frac{\Delta t}{(\Delta y)^2}\left(h_{i,j+1}^n - 2h_{i,j}^n + h_{i,j-1}^n\right) - \frac{\Delta t}{\Delta y}\left(J^*_{i,j+\frac{1}{2}} - J^*_{i,j-\frac{1}{2}}\right) - \Delta t \varepsilon_y h_{i,j}^n + \Delta t \frac{\rho_w}{\rho_p} p \tag{11}$$

where superscript denotes time step, subscript denotes spatial grid number, p is snow precipitation (m/s), ρ_w is density of water (1000 kg/m^3), Δt is time increment, Δx and Δy are the spatial resolution, and J^* is snow particle

flux due to advection. The snow particle flux of the advection term in equation (11) between computational cells may be computed as,

$$J^*_{i+1/2,j} = \begin{cases} \varphi_x \tilde{h}^{\mathrm{W}}_{i+1/2,j} \; ; \varphi_x \geq 0 \\ \varphi_x \tilde{h}^{\mathrm{E}}_{i+1/2,j} \; ; \varphi_x < 0 \end{cases}$$
$$J^*_{i,j+1/2} = \begin{cases} \varphi_y \tilde{h}^{\mathrm{S}}_{i,j+1/2} \; ; \varphi_y \geq 0 \\ \varphi_y \tilde{h}^{\mathrm{N}}_{i,j+1/2} \; ; \varphi_y < 0 \end{cases} \tag{12}$$

where $\tilde{h}$ is the modified surface elevation with the flux limiter Φ, L and R refer to the left and right sides at the computational cell i. The positive sign in superscript means effective when the wave velocity φ is positive while the negative sign in superscript means effective when the wave velocity φ is negative. The limiters are required to eliminate numerical oscillations. Based on the MUSCL scheme, the interface values can be expressed as a linear extrapolation of the average values at the two upwind cells. They can be computed as

$$\tilde{h}^{\mathrm{W}}_{i+1/2,j} = h_{i,j} + \frac{1}{2}\Phi^{+}_{i-\frac{1}{2},j}\left(h_{i,j} - h_{i-1,j}\right), \qquad \tilde{h}^{\mathrm{E}}_{i+1/2,j} = h_{i+1,j} - \frac{1}{2}\Phi^{-}_{i+\frac{3}{2},j}\left(h_{i+2,j} - h_{i+1,j}\right),$$
$$\tilde{h}^{\mathrm{S}}_{i,j+1/2} = h_{i,j} + \frac{1}{2}\Phi^{+}_{i,j-\frac{1}{2}}\left(h_{i,j} - h_{i,j-1}\right), \qquad \tilde{h}^{\mathrm{N}}_{i,j+1/2} = h_{i,j+1} - \frac{1}{2}\Phi^{-}_{i,j+\frac{3}{2}}\left(h_{i,j+2} - h_{i,j+1}\right), \tag{13}$$

and

$$\Phi^{+}_{i-1/2} = \Phi(r^{+}_{i-1/2}), \qquad \Phi^{-}_{i+1/2} = \Phi(r^{-}_{i+1/2}). \tag{14}$$

The ratio between successive gradients, *r*, can be estimated by

$$r^{+}_{i-\frac{1}{2},j} = \frac{h_{i+1,j}-h_{i,j}}{h_{i,j}-h_{i-1,j}}, \qquad r^{-}_{i+\frac{3}{2},j} = \frac{h_{i,j}-h_{i+1,j}}{h_{i+1,j}-h_{i+2,j}},$$
$$r^{+}_{i,j-\frac{1}{2}} = \frac{h_{i,j+1}-h_{i,j}}{h_{i,j}-h_{i,j-1}}, \qquad r^{-}_{i,j+\frac{3}{2}} = \frac{h_{i,j}-h_{i,j+1}}{h_{i,j+1}-h_{i,j+2}}. \tag{15}$$

Through comparisons among the flux limiters, Van Leer's (Van Leer, 1974), min-mod (Roe, 1986), superbee (Roe and Baines, 1982), and MUSCL limiter (Van Leer, 1979), the MUSCL limiter showed the best performance for bell shape solutions. Thus, the MUSCL limiter was selected in this study. The MUSCL limiter (Van Leer, 1979) can be expressed as,

$$\Phi(r) = \max[0, \min(2r, (r+1)/2, 2)]. \tag{16}$$

This numerical algorithm was implemented in the Snow Movement Over Open Terrain for Hydrology (SMOOTH) model platform (Ohara, 2014).

RESULTS

The numerical solutions were verified by the one-dimensional analytical solution, Equation (8), around a snow fence. Figure 5 shows the two demonstrative simulation results and the corresponding analytical solutions. The discrepancies were measured by the root mean standard difference (RMSD) and the Nash–Sutcliffe model efficiency (NSME), inserted in the graphs. The differences were very small although a slightly larger error is expected in the negative erosion case (eddy case) in the left panel. It can be concluded that the numerical algorithm presented above effectively resists the anticipated convective instability without introducing numerical diffusivity.

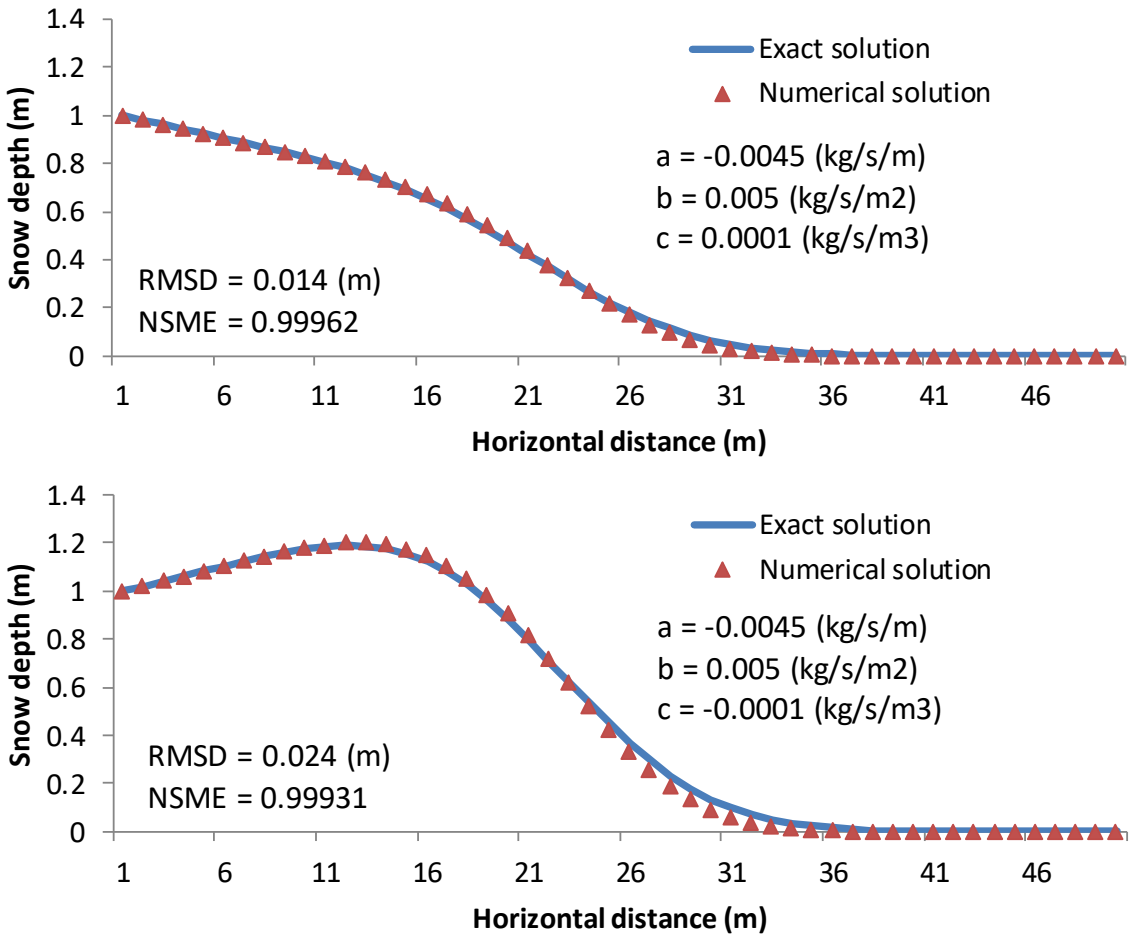

Figure 5. Validation of the numerical algorithm for the LPD equation

The numerical algorithm was intended to test the LPD equation for two-dimensional and more complexed terrain. The demonstrative preliminary model output around the thermokarst lakes (N70.7058218, W153.9254947) in Alaska is shown in Figure 6. The terrain model was prepared using the National Elevation Database (NED, Gesch et al., 2002) digital elevation model (DEM), and northwest wind was assumed. This preliminary result was based on the model parameters found in the Rocky Mountains, a = -0.0045, b = 0.00014, c = 0; therefore, they may not be realistic. Nevertheless, the simulated snow accumulation pattern makes sense as seasonal snow typically develops along the lakeshore in this region. This LPE model (SMOOTH) can interpolate and possibly extrapolate the observed seasonal snow distributions over any windy open areas.

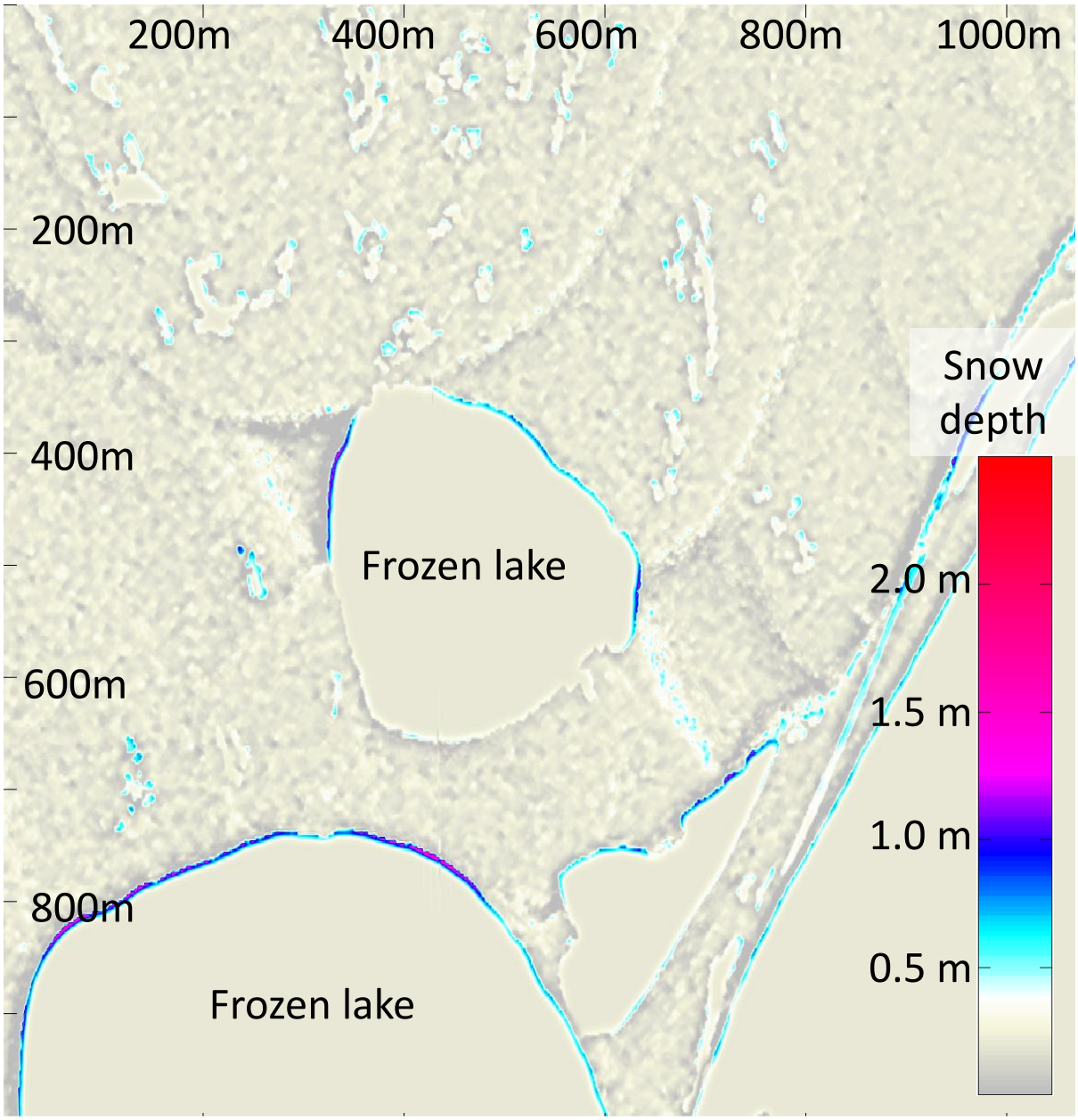

Figure 6. Preliminary spatial model application output of the LPD model (SMOOTH5)

CONCLUSIONS

The linear theory is convenient and useful to analyze the particle transport and deposition system within a flow because the exact solutions can be obtained with an appropriate boundary condition. This presentation demonstrated the real applications of the LPD theory in a two-dimensional field using the MUSCL numerical scheme. This theory assumed the linearity, which implies that the model parameters, diffusion, drift, and erosion coefficients must be independent from the relative height of the surface, *h*. However, the effects of non-linear motion and mass gain and loss can be evaluated separately, and added to the solutions of the linear system equation because of the superposition principle. This efficient numerical algorithm made the LPD equation ready for application in any open terrain. However, much study is needed to determine the snow particle motion parameters (dispersion, advection, and erosion coefficients) especially around the vegetation or any surface roughness.

ACKNOWLEDGEMENT

This study was supported by the National Science Foundation under award no. EPS-1208909.

REFERENCES

Essery, R. L. H., L. Li, and J.W. Pomeroy. 1999. A Distributed Model of Blowing Snow over Complex Terrain. *Hydrol. Process.*, 13, 2423–2438.

Gesch, D., Oimoen, M., Greenlee, S., Nelson, C., Steuck, M., and Tyler, D. 2002. The national elevation dataset. Photogrammetric Engineering and Remote Sensing, 68(1), 5-32.

Greene, E.M., G.L. Liston, and R.A. Pielke. 1999. Simulation of above treeline snowdrift formation using a numerical snow-transport model. *Cold Reg. Sci. Technol.*, 30(1–3), 135–144.

Lehning, M., I. Völksch, D. Gustafsson, T.A. Nguyen, M. Stähli, and M. Zappa. 2006. ALPINE3D: a detailed model of mountain surface processes and its application to snow hydrology. *Hydrological Processes*, 20(10), 2111-2128.

Liston, G.E., R.B. Haehnel, M. Sturn, C.A. Hiemstra, S. Berezovskaya, and R.D. Tabler. 2007. Instruments and Methods Simulating complex snow distributions in windy environments using SnowTran-3D. Journal of Glaciology, vol. 53, Issue 181, 241-256.

Mott, R. and M. Lehning. 2010. Meteorological modeling of very high-resolution wind fields and snow deposition for mountains. *J. Hydrometeorol*. 11 (4), 934–949.

Ohara, N. 2014. A practical formulation of snow surface diffusion by wind for watershed scale applications. Water Resources Research, 50(6):5074-5089.

Ohara, N. 2017. An Eulerian equation for snow accumulation downstream of an object. Water Resources Research, 53(2):1525-1538.

Pomeroy, J.W., D.M. Gray, and P.G. Landine. 1993. The Prairie Blowing Snow Model - characteristics, validation, operation. *J. Hydrol*., 144, 165–192.

Roe, P. 1986. Characteristic-based schemes for the euler equations. Annual review of fluid mechanics, 18(1):337-365.

Roe, P. and M. Baines. 1982. Algorithms for advection and shock problems. In Numerical Methods in Fluid Mechanics, pages 281-290.

Tabler, R. D. 2003. *Controlling blowing and drifting snow with snow fences and road design* (No. NCHRP Project 20-7 (147)).

Van Leer, B. 1974. Towards the ultimate conservative difference scheme. ii. Monotonicity and conservation combined in a second-order scheme. Journal of computational physics, 14(4):361-370.

Van Leer, B. 1979. Towards the ultimate conservative difference scheme. v. a second-order sequel to Godunov's method. Journal of computational Physics, 32(1):101-136.